Orbital ordering as the determinant for ferromagnetism in biferroic $BiMnO_3$

A. Moreira dos Santos and A. K. Cheetham
Materials Department, University of California, Santa Barbara, California 93106-5050

T. Atou, Y. Syono, Y. Yamaguchi, K. Ohoyama, and H. Chiba
IMR, Tohoku University, Katahira 2-1-1, Aoba-ku, Sendai 980-8577, Japan

C. N. R. Rao
Chemistry and Physics of Materials Unit, Jawaharlal Nehru Center for Advanced Scientific Research, Bangalore 560 064, India

(Received 28 March 2002; revised manuscript received 19 June 2002; published 20 August 2002)

The ferromagnetic structure of $BiMnO_3$, $T_c = 105$ K, has been determined from powder neutron-diffraction data collected at 20 K on a sample synthesized at high pressures using a cubic anvil press. $BiMnO_3$ is a distorted perovskite that crystallizes in the monoclinic space group $C2$ with unit-cell parameters $a = 9.5317(7)$ Å, $b = 5.6047(4)$ Å, $c = 9.8492(7)$ Å, and $ß = 110.60(1)°$ ($Rp = 6.78\%$, $wRp = 8.53\%$, reduced $\chi^2 = 1.107$). Data analysis reveals a collinear ferromagnetic structure with the spin direction along [010] and a magnetic moment of $3.2\mu B$. There is no crystallographic phase transition on cooling the polar room-temperature structure to 20 K, lending support to the belief that ferromagnetism and ferroelectricity coexist in $BiMnO_3$. Careful examination of the six unique Mn-O-Mn superexchange pathways between the three crystallographically independent Mn^{3+} sites shows that four are ferromagnetic and two are antiferromagnetic, thereby confirming that the ferromagnetism of $BiMnO_3$ stems directly from orbital ordering.

DOI: 10.1103/PhysRevB.66.064425 PACS number(s): 75.50.Dd, 75.25.+z, 77.84.Dy

I. INTRODUCTION

The remarkable magnetoelectric properties of $BiMnO_3$ have attracted considerable attention during the last three years. It is well established that $BiMnO_3$ becomes ferromagnetically ordered on cooling below 110 K,[1–3] and there is good reason to believe that the ferromagnetism coexists with ferroelectricity. This is to be contrasted with the behavior of the analogous $LaMnO_3$, which orders antiferromagneticaly at 150 K.[4] Such biferroic behavior is very rare in a single phase material.[5–7] The evidence for ferroelectricity, however, has largely been based upon informed speculation,[8] although a structure determination by powder diffraction has indicated that the space group at room temperature is $C2$,[9] which would be consistent with ferroelectricity. The reason for the uncertainty in this area is that the preparation of bulk $BiMnO_3$ requires high pressures and temperature, so it is difficult to make large samples of high quality material. However, evidence for magnetoelectric behavior has recently been garnered from measurements on thin films and impure bulk samples, both of which show ferroelectric hysterisis loops below the Curie temperature.[10] The low-temperature crystal and magnetic structures of $BiMnO_3$ have not been reported, but would shed further light on the coexistence of ferroelectricity and ferromagnetism. In the present work, we describe the determination of the crystal and magnetic structures of $BiMnO_3$ from a low-temperature, powder neutron-diffraction study.

II. EXPERIMENT

The preparation of a polycrystalline sample of $BiMnO_3$ was carried out using a cubic anvil press at 973 K and 6 GPa, as reported previously.[9] Powder neutron-diffraction data were collected on the Hermes diffractometer on the JRR-3M facility at the Japan Atomic Energy Research Institute with a mean neutron wavelength of 1.8196 Å. Data were analyzed by Rietveld refinement using the GSAS suite of programs.[11] Neutron-scattering lengths of 8.531, −3.730, and $5.803(10^{-15}$ m) were used for Bi, Mn, and O, respectively. The magnetic form factor of Mn^{3+} was based upon the free-ion calculations of Watson and Freeman.[12]

III. RESULTS AND DISCUSSION

A careful comparison between the high angle portions of the neutron-diffraction data collected at 20 K and room temperature[9] revealed no evidence for a structural phase

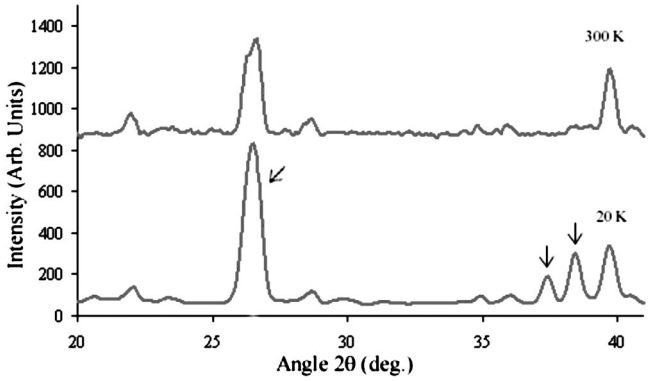

FIG. 1. A comparison of the low angle regions of the neutron powder-diffraction pattern of $BiMnO_3$ at 300 and 20 K. Note the appearance of additional reflections at 20 K due to the onset of ferromagnetic ordering.

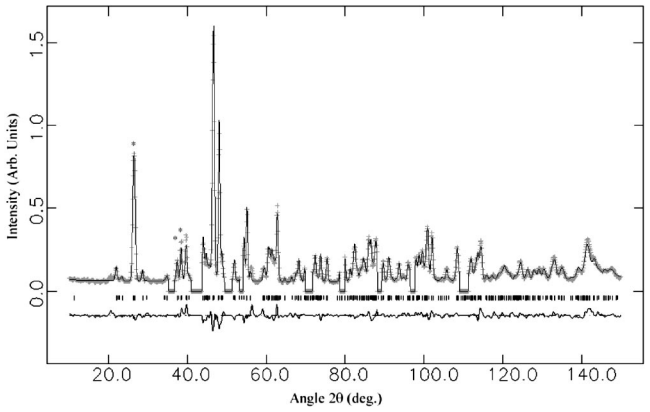

FIG. 2. Observed (dots) and calculated (line) profile of $BiMnO_3$ at 20 K. A difference curve is also shown. The magnetic peaks are indicated by an asterisk.

transition on cooling to low temperatures. The crystal structure of $BiMnO_3$ at 20 K was therefore refined using the room-temperature structure in space group $C2$ as a starting model. The low angle portion of the pattern ($<40°\ 2\theta$), however, contained a small number of magnetic Bragg reflections that could be indexed on the basis of the crystallographic unit cell; the most intense features are the (-202), (-113), (311), and (202) reflections (see Fig. 1). These observations are consistent with the onset of ferromagnetic ordering, and we attempted to model the intensities of these magnetic peaks on the basis of a variety of plausible collinear spin models. An excellent fit was obtained with a model in which the spin vector was aligned along the unique [010] axis of the monoclinic crystal structure, and a full Rietveld refinement of the crystal and magnetic structure was carried out on this basis (see Fig. 2 and Table I). Lines from small amounts of impurity phases were excluded from the analysis. One of the impurity phases was identified as $Bi_2(CO)_3O_2$; the identity of the second phase could not be established. Isotropic temperature factors for each atom type were constrained to be equal. The refined magnetic moment was found to be 3.2(3) μB, which is in the expected range for a high spin d^4 Mn^{3+} ion and consistent with the previously reported magnetization curve of $BiMnO_3$ measured at 5 K.[13]

TABLE I. Refined structural parameters for $BiMnO_3$ at 20 K. Space group $C2$, $a=9.5317(7)$ Å, $b=5.6047(4)$ Å, $c=9.8492(7)$ Å, $ß=110.60(1)°$, $V=492.54(7)$ Å^3. There were 1249 observations. $Rp=6.78\%$, $wRp=8.53\%$. Reduced $\chi^2=1.107$ for 20 variables.

Atom	x	y	z	$Ui/Ue*100$
Bi(1)	0.136(1)	0.004(7)	0.373(1)	0.4
Bi(2)	0.363(1)	0.068(8)	0.116(1)	0.4
Mn(1)	0	0	0	0.25
Mn(2)	0.250(4)	0.036(9)	0.754(3)	0.25
Mn(3)	0.5	0.078(4)	0.5	0.25
O(1)	0.092(2)	−0.025(9)	0.834(2)	0.9
O(2)	0.397(2)	0.128(8)	0.673(2)	0.9
O(3)	0.139(2)	0.367(8)	0.622(2)	0.9
O(4)	0.355(2)	0.316(8)	0.420(2)	0.9
O(5)	0.300(2)	0.225(8)	0.907(2)	0.9
O(6)	0.154(2)	0.225(8)	0.115(2)	0.9

TABLE II. Selected bond lengths for $BiMnO_3$ at 20 K.

Mn1–O1	2.11(1)×2	Mn2–O1	1.97(4)
Mn1–O5	2.08(4)×2	Mn2–O2	1.90(4)
Mn1–O6	1.97(3)×2	Mn2–O3	2.30(4)
Mn3–O2	2.27(1)×2	Mn2–O4	2.06(3)
Mn3–O3	1.86(4)×2	Mn2–O5	1.82(3)
Mn3–O4	1.88(4)×2	Mn2–O6	2.17(4)
Bi1–O1	2.43(1)	Bi2–O1	2.36(2)
Bi1–O2	2.16(2)	Bi2–O1'	3.02(2)
Bi1–O3	2.25(1)	Bi2–O2	2.53(2)
Bi1–O3'	3.20(2)	Bi2–O3	2.83(2)
Bi1–O4	2.29(2)	Bi2–O5	2.17(1)
Bi1–O4'	2.64(2)	Bi2–O5'	2.74(2)
Bi1–O4''	3.06(1)	Bi2–O5''	2.95(1)
Bi1–O5	3.21(1)	Bi2–O6	2.18(1)
Bi1–O6	3.20(1)	Bi2–O6'	2.87(2)

Selected bond lengths and bond angles for $BiMnO_3$ are given in Tables II and III, and the coordination environments for the Bi and Mn atoms are shown in Figs. 3 and 4, respectively. The BiO_n polyhedra are unsymmetrical as a consequence of the stereochemical activity of the lone pairs of electrons on the Bi^{3+} ions. This asymmetry is believed to be the major driving force behind the ferroelectric properties of $BiMnO_3$, as it is in the behavior of $Pb(Zr_xTi_{1-x})O_3$ (PZT) and related phases. In both $BiMnO_3$ and PZT for example, the A cations are displaced approximately along the body diagonal of the cubic perovskite subcell. The fact that there is no structural phase transition and that the distortions remain substantially the same on cooling from room temperature to 20 K lends strong support to the belief that $BiMnO_3$ remains ferroelectric in the ferromagnetic phase.

TABLE III. Selected bond angles for $BiMnO_3$ at 20 K.

O1–Mn1–O1	172.5(3)	O1–Mn2–O2	174.1(3)
O1–Mn1–O5	91.2(1)	O1–Mn2–O4	90.7(2)
O1–Mn1–O5	83.2(1)	O1–Mn2–O5	90.9(2)
O1–Mn1–O6	93.4(1)	O1–Mn2–O6	80.9(1)
O1–Mn1–O6	91.5(1)	O2–Mn2–O4	91.8(2)
O1–Mn1–O5	83.2(1)	O2–Mn2–O5	86.8(2)
O1–Mn1–O5	91.2(1)	O2–Mn2–O6	104.4(2)
O1–Mn1–O6	91.5(1)	O4–Mn2–O5	177.8(3)
O1–Mn1–O6	93.4(1)	O4–Mn2–O6	89.6(2)
O5–Mn1–O5	84.6(2)	O5–Mn2–O6	89.1(1)
O5–Mn1–O6	170.7(2)	O3–Mn3–O3	101.5(3)
O5–Mn1–O6	87.9(1)	O3–Mn3–O4	165.8(1)
O5–Mn1–O6	87.9(1)	O3–Mn3–O4	85.8(7)
O5–Mn1–O6	170.7(2)	O3–Mn3–O4	85.8(7)
O6–Mn1–O6	100.0(2)	O3–Mn3–O4	165.8(1)
		O4–Mn3–O4	89.7(2)

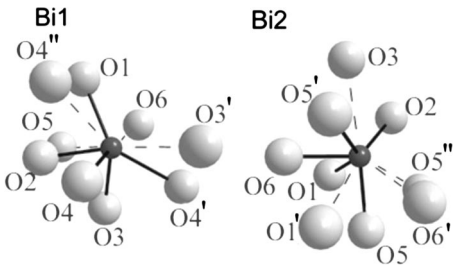

FIG. 3. Coordination environments of Bi1 and Bi2; showing the shortest distances in bold and longer ones in dashed lines.

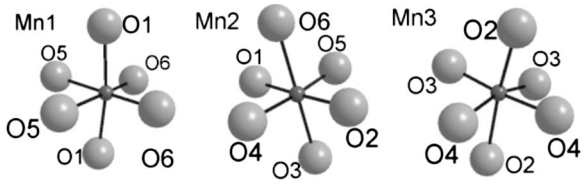

FIG. 4. Coordination environment of the Jahn-Teller distorted Mn cations; see Tables II and III.

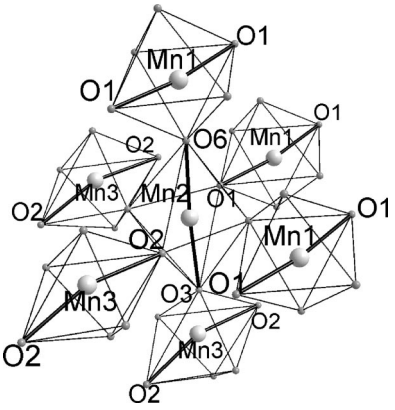

FIG. 5. Three-dimentional magnetic exchange between the Mn atoms; the thick lines correspond to the occupied d_{z^2} orbitals.

TABLE IV. Primary superexchange interactions in $BiMnO_3$ at 20 K. The bond angle estimated standard deviations are $\sim 0.3°$.

Pathway	Angle°	Interaction
Mn(1)–O(1)–Mn(2)	154.8	FM
Mn(2)–O(2)–Mn(3)	147.0	FM
Mn(2)–O(3)–Mn(3)	160.4	FM
Mn(2)–O(4)–Mn(3)	148.8	AFM
Mn(1)–O(5)–Mn(2)	149.5	AFM
Mn(1)–O(6)–Mn(2)	158.7	FM

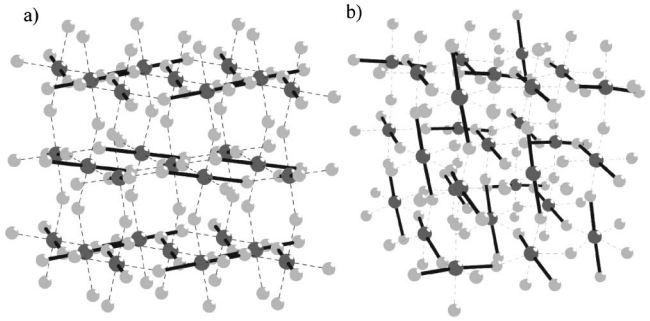

FIG. 6. The two-dimensional orbital ordering in (a) $LaMnO_3$ is compared with the three-dimensional orbital ordering seen in (b) $BiMnO_3$. Bold lines represent the orientation of the d_{z^2} orbitals, as revealed by the elongations of the MnO_6 octahedra.

Each of the three MnO_6 polyhedra shows the axial elongation that is typical of Jahn-Teller distorted d^4 cations in perovskite systems. The orbital ordering that is associated with these distortions in $BiMnO_3$ is the same as that observed at room temperature (Fig. 5), resulting in superexchange interactions that are largely ferromagnetic (Table IV). In four of the six pathways, the orbital ordering ensures that half filled d_{z^2} orbitals point towards the empty $d_{x^2-y^2}$ orbitals on the next manganese; such interactions are predicted to be ferromagnetic according to the rules proposed by Goodenough[14,15] and Kanamori;[16] they are strongest when the *M-O-M* bond angle is close to 180°. We note that three of the four ferromagnetic Mn-O-Mn angles are significantly larger than the antiferromagnetic ones (Table IV). There is no instance in which a half filled d_{z^2} orbital points towards another half filled d_{z^2} orbital (this would be strongly antiferromagnetic), but two cases in which empty $d_{x^2-y^2}$ orbitals point towards each other [through O(4) and O(5)]. Optimally, these interactions would be weakly antiferromagnetic, but this cannot be accommodated in combination with the constraints of the strong ferromagnetic interactions, so the system must be slightly frustrated.

It is interesting to compare the ferromagnetic structure of $BiMnO_3$ with the *A*-type antiferromagntic structure found in the related perovskite, $LaMnO_3$. This comparison has recently been discussed by Hill and Rabe[17] and Woo *et al.*[18] $LaMnO_3$ is also orbitally ordered,[19] but in a simple manner which leads to ferromagnetic sheets that are antiferromagnetically aligned with respect to each other. Half filled d_{z^2} orbitals point towards empty $d_{x^2-y^2}$ orbitals within the ferromagnetic sheets, but this results in empty $d_{x^2-y^2}$ orbitals facing each other via the oxygens between the sheets, leading to the overall antiferromagnetic structure (see Fig. 6). It is the substitution of La by Bi that is responsible for stabilizing a different structural distortion with different orbital ordering that leads to ferromagnetism. There are several factors that may be responsible for this crucial difference. The greater covalence of the Bi-O bonds compared with La-O bonds will have an impact on the Mn-O-Mn interactions. Second, the bismuth lone pairs lead to *A* cations displacements along the $\langle 111 \rangle$ directions of the cubic perovskite sub-

cell that are imcompatible with the two-dimensional orbital ordering found in $LaMnO_3$. The more complex orbital ordering pattern found in $BiMnO_3$, which must stem from the distortions imposed by the Bi lone pairs, leads to three-dimensional ferromagnetic interactions that result in the observed spin structure.

ACKNOWLEDGMENTS

The work was supported by the MRSEC Program of the National Science Foundation under Award No. DMR00-80034. A. Moreira dos Santos wishes to thank Dr. Angus Lawson for help with the magnetic refinement.

[1] I. Troyachuk, N.V. Samsonenko, E.F. Shapovalova, I.M. Kolesova, and H. Shymczak, J. Phys.: Condens. Matter **8**, 11 205 (1996).
[2] F. Sugawara, S. Iida, Y. Syono, and S.-i. Akimoto, J. Phys. Soc. Jpn. **20**, 1529 (1965).
[3] V. Bokov, I.E. Myl'nikova, S.A. Kizaev, M.F. Bryzhina, and N.A. Grigoryan, Fiz. Tverd. Tela (Leningrad) **7**, 2993 (1966) [Sov. Phys. Solid State **7**, 2993 (1966)].
[4] C.N.R. Rao, A.K. Cheetham, and R. Mahesh, Chem. Mater. **8**, 2421 (1996).
[5] N. Hill, J. Phys. Chem. B **104**, 6694 (2000).
[6] H. Schmidt, Ferroelectrics **162**, 317 (1994).
[7] S. Skinner, IEEE Trans. Parts Mater. Packag. **6**, 68 (1970).
[8] V. Bokov, N. Grigoryan, M. Bryzhina, and V. Kazary, Izv. Akad. Nauk Arm. SSR, Fiz. **33**, 1164 (1969).
[9] T. Atou, H. Chiba, K. Ohoyama, Y. Yamaguchi, and Y. Syono, J. Solid State Chem. **145**, 639 (1999).
[10] A. Moreira dos Santos, S. Parashar, A.R. Raju, A.K. Cheetham, and C.N.R. Rao, Solid State Commun. **122**, 49 (2002).
[11] A. Larson and R.B. von Dreele, GSAS Manual, 1986.
[12] R. Watson and A. Freeman, Acta Crystallogr. **14**, 27 (1961).
[13] H. Chiba, T. Atou, and Y. Syono, J. Solid State Chem. **132**, 139 (1997).
[14] J.B. Goodenough, Phys. Rev. **100**, 564 (1955).
[15] J.B. Goodenough, J. Phys. Chem. Solids **6**, 287 (1958).
[16] J. Kanamori, J. Phys. Chem. Solids **10**, 87 (1959).
[17] N.A. Hill and K. Rabe, Phys. Rev. B **59**, 8759 (1999).
[18] H. Woo, T.A. Tyson, M. Croft, S.-W. Cheong, and J.C. Woicik, Phys. Rev. B **63**, 134412 (2001).
[19] L.E. Gonchar and A.E. Nikiforov, Fiz. Tverd. Tela (St. Petersburg) **42**, 1070 (2000) [Phys. Solid State **42**, 1070 (2000)].